Molecular Human Reproduction Vol.13, No.12 pp. 837–844, 2007
Advance Access publication on November 2, 2007 doi:10.1093/molehr/gam076

Analysis of replication protein A (RPA) in human spermatogenesis

Maria Oliver-Bonet[1], Mercedes Campillo[2], Paul J. Turek[3,4,5], E. Ko[1] and R.H. Martin[1,6]

[1]Department of Medical Genetics, University of Calgary, 3330 Hospital Drive NW, Calgary, Alberta, Canada T2N 4N1; [2]Laboratori de Medicina Computacional, Unitat de Bioestadística, Facultat de Medicina, Universitat Autònoma de Barcelona, 08193 Bellaterra, Spain; [3]Department of Urology, University of California San Francisco, San Francisco, CA 94143-1695, USA; [4]Department of Obstetrics and Gynecology, University of California San Francisco, San Francisco, CA 94143-1695, USA; [5]Department of Reproductive Sciences, University of California San Francisco, San Francisco, CA 94143-1695, USA

[6]Correspondence address. E-mail: rhmartin@ucalgary.ca

Replication protein A (RPA) has been identified as a component of early recombination nodules. It is thought to stimulate homologous pairing and strand exchange reactions. The expression pattern of RPA in human spermatocytes has been analysed using immunocytogenetic techniques on testicular biopsies from adult male patients. What appears to be connecting RPA-filaments was observed between as yet unsynapsed homologous regions at early stages of zygotene. RPA foci were also observed in synaptic segments at zygotene and early pachytene, in numbers that peak at the end of zygotene. The presence of a localization pattern for RPA was also detected, but statistical analysis of distances between adjacent RPA foci shows that this pattern does not always follow a gamma distribution. Finally, it was determined that RPA is absent from non-centromeric heterochromatin in chromosome 9. The observed bridge-like structure could be the visualization of a proposed pre-synaptic RPA role in the strand invasion that precedes the formation of a Holliday Junction. These observations strengthen the original pre-synaptic model, although the visualization of post-synaptic RPA foci may indicate the presence of a different role for this protein during homologous recombination.

Keywords: human spermatogenesis; meiosis; meiotic recombination; RPA

Introduction

Meiotic recombination results from the repair of DNA double-strand breaks (DSBs) introduced by the Spo11 protein (Keeney *et al*., 1997; Romanienko and Camerini-Otero, 2000; Henderson and Keeney, 2004). It is a highly regulated process, and several proteins have been described as essential for the proper progression of recombination. The repair of the DSBs occurs in several steps, including end-resection, homology search, strand invasion and exchange, heteroduplex formation and resolution. The process promotes the use of non-sister chromatids of homologous chromosomes as templates for repair, rather than sister chromatids.

Homology search is preceded by the pairing of homologous chromosomes. Once homologues are paired, a sequence-specific check for homology is initiated. It has been proposed that proteins present in early recombination nodules (ENs) facilitate this process (Carpenter, 1987). Identification of proteins implicated in the formation of ENs in mammalian prophase nuclei has been performed using immunostaining techniques (Barlow *et al*., 1997; Plug *et al*., 1997; Moens *et al*., 1999). The temporal and functional relationships between these proteins have been the focus of recent studies in different organisms (Plug *et al*., 1998; Moens *et al*., 2002; Oliver-Bonet *et al*., 2005). Replication protein A (RPA) has been identified as a component of ENs (Plug *et al*., 1997; Walpita *et al*., 1999). RPA is a heterotrimeric protein that binds with high affinity to single-stranded DNA (ssDNA). It is required for several metabolic processes, including DNA replication, repair and recombination, and is essential for survival of the cell.

In vitro experiments have shown that RPA stimulates homologous pairing and strand exchange reactions catalysed by RAD51 (Eggler *et al*., 2002). A proposed model suggests that during homologous recombination, RPA binds the 3′ ssDNA resultant from 5′ end resection of DSBs. This binding would facilitate the binding of RAD51 to ssDNA via the removal of the DNA secondary structure that results from DSB resection (Sugiyama *et al*., 1997). As a consequence, a nucleoprotein filament containing RAD51 would be formed. The role of this filament is to initiate the homology-driven invasion of the DNA strand into the homologous double-strand DNA partner.

During meiosis, RPA has been described to appear somewhat later in time than RAD51 foci, on already synapsed segments of synaptonemal complexes (SCs) at zygotene (Plug *et al*., 1998; Moens *et al*., 2002; Oliver-Bonet *et al*., 2005). However, RPA has occasionally been detected in asynaptic regions at early pachytene (Oliver-Bonet *et al*., 2005), although it is absent in the asynaptic heterochromatic region of the Y chromosome. This last characteristic is not specific to humans, as it has also been described in the mouse (Moens *et al*., 2002). This observation suggests that RPA could play a different role during meiotic recombination.

The present study was designed to further explore the presence of RPA foci in asynaptic regions, as well as the absence of this protein

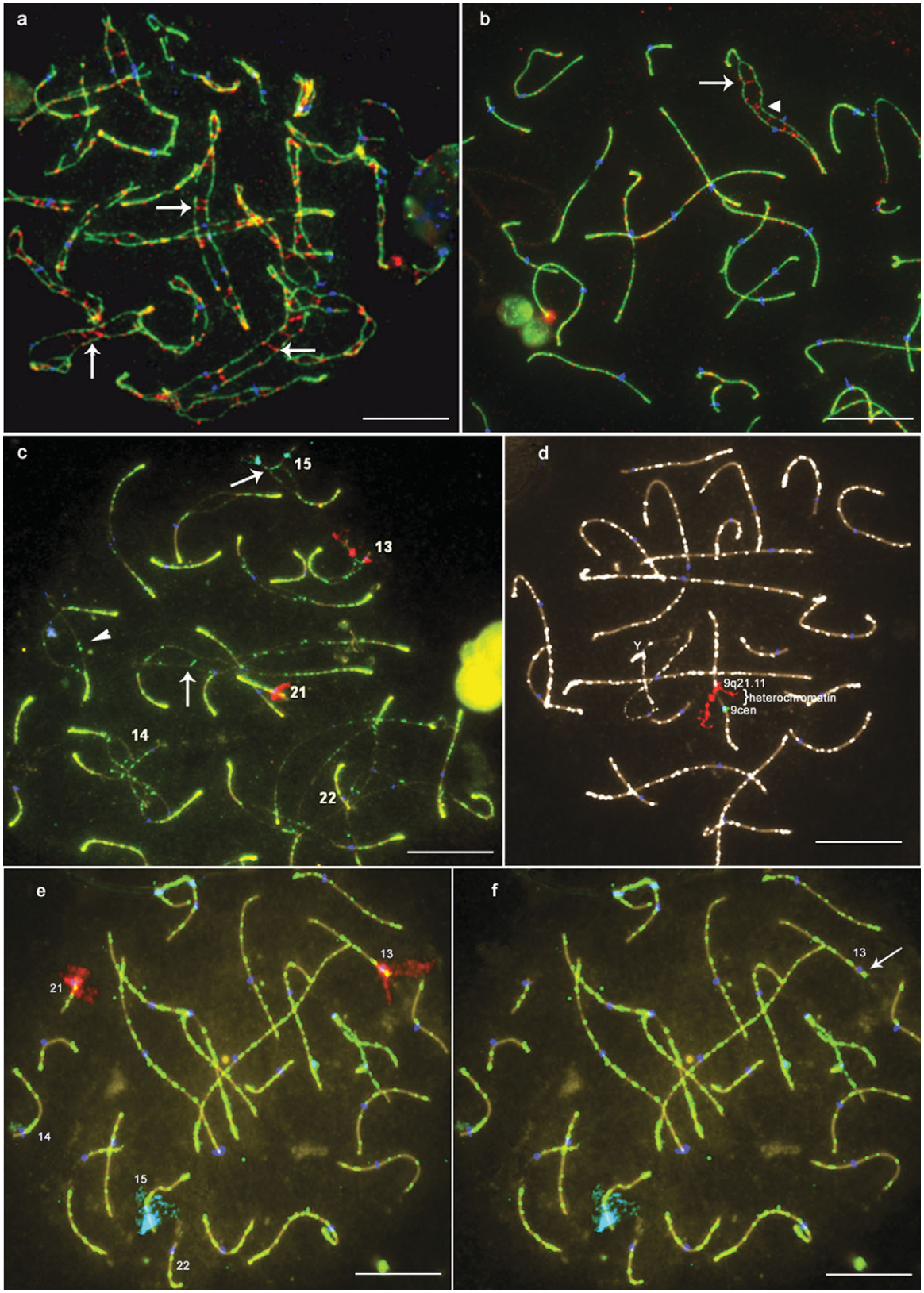

Figure 1: RPA expression in human spermatocytes (**a–c**) and RPA distribution analysis (**d–f**)
SMC3 protein (cohesion axis) is shown in green (a and b), SCPY3 and SCPY1 proteins (SC proteins) are shown in brown (c–f), centromeres in blue and RPA protein in red (a and b), in green (c, e and f) and in white (d). RPA bridge-like structures are visible between as yet unsynapsed homologous SCs at early zygotene (a, arrows) and at late zygotene on some SCs that are delayed in the synaptic process (b, arrow). Some RPA bridge-like structures appear to pull the two homologues together (b, arrowhead; c, arrow). RPA is absent from the heterochromatic regions of chromosomes Y and 9. Chromosome 9 heterochromatin has been delimited with the combined use of a centromeric probe (d, green signal) and a BAC probe targeting the band immediately adjacent to the heterochromatic region (d, red signal). Acrocentric chromosomes have been identified by FISH [SCs 13, 21 (Cy3) and 15 (Spectrum Aqua)] and by size and morphology (SCs 14 and 22) (e). (f) corresponds to (e) without the red FISH signals. Some RPA foci have been detected in the p arm of acrocentric chromosomes (f, arrow). White bar corresponds to 10 μm.

from other non-centromeric heterochromatic regions of autosomal chromosomes. Gamma distribution was used to detect the presence of interference in the distribution of distances between adjacent RPA foci. This model has been used in other studies for estimating the strength of interference (McPeek and Speed, 1995; de Boer *et al*., 2006). Our findings support the idea of a pre-synaptic role for RPA, show that RPA does not bind to the non-centromeric heterochromatic region of chromosome 9 and, although similarities with Mut L homolog 1 (MLH1) distribution have been observed, indicate that RPA localization along the SCs does not always display interference.

Materials and Methods

Testicular tissues were obtained from three patients ascertained for reasons unrelated to meiotic defects. One testicular biopsy was obtained from an orchiectomy performed for testicular cancer. The other two were obtained from fine needle aspiration (Turek *et al*., 2000) in fertile men undergoing vasovasostomy, recruited from the University of California San Francisco, San Francisco, CA, USA. Testicular tissue was kept in phosphate-buffered saline (PBS), on ice, until use. Written consent was obtained from all patients and the study was approved by our Institutional Review Board.

SC spreading and immunolabelling

Meiotic spreads were obtained using a protocol described previously (Sun *et al*., 2004). Blocking reagent (4–5% donkey serum in PBS with 0.1% Triton X) was applied to the slides to prepare the spermatocytes for immunolabelling. Primary antibodies were used to detect proteins of the central and lateral elements of the synaptonemal complex [mouse synapsin 1 (SYN1) (1:1000), a gift from P. Moens, York University, and goat synaptoremal complex protein 3 (SCP3) (1:500), a gift from T. Ashley, Yale University, respectively], proteins of the centromere [human CREST (1:250), a gift from M. Fritzler, University of Calgary], of the cohesion complex [rabbit structural maintenance of chromosomes (SMCs) 3 (1:500), abcam antibodies, UK] and RPA protein [goat RPA (1:250), Santa Cruz technologies, Inc., Santa Cruz, CA, USA]. A cocktail of secondary fluorescent antibodies was used to detect the primary antibodies. The structural elements of the synaptonemal complex were detected using AlexaFluor555-labelled donkey anti-goat (Molecular Probes, Inc., OR, USA) and Cy3-labelled donkey anti-mouse antibodies (Jackson Immunoresearch, West Grove, PA, USA). Centromeres were detected using AMCA-labelled donkey anti-human IgG (Jackson Immunoresearch, West Grove, PA, USA). SMC3 protein was detected using AlexaFluor488-labelled donkey anti-rabbit (Molecular Probes, Inc.) and RPA was detected using either AlexaFluor555- or AlexaFluor488-labelled donkey anti-goat (Molecular Probes, Inc.). Slides were mounted in *p*-phenylenediamine antifade, and a Zeiss Axiophot fluorescent photomicroscope attached to Applied Imaging Cytovision 3.1 software (Applied Imaging Corporation, Santa Clara, CA, USA) was used to capture and analyse the spermatocyte nuclei.

Analysis of MLH1 distribution was made on testicular samples of five fertile (vasovasostomy) controls, as part of a different analysis performed in our lab. A polyclonal antibody against the MLH1 protein was used to detect MLH1 (Oncogene, San Diego, CA, USA).

Fish analysis

Identification of acrocentric chromosomes for RPA analysis was performed using centromeric probes for chromosome 15 [pTRA-20, kindly provided by K.H. Choo, (Choo *et al*., 1990) DEAC aqua] and chromosomes 13 and 21 (Cytocell, Cambridge, UK, Cy3). Identification of chromosomes 14 and 22 was made by size, morphology and elimination of the other D and G group chromosomes, when possible. Chromosome 9 was identified with the use of a centromeric probe (Vysis Inc., Downer's Grove, IL, USA, SpectrumGreen), and BAC probe RP11-203L2 (9q21.11, Spectrum Orange) was used to delimit the heterochromatic region. All hybridizations were performed using a microwave protocol (Ko *et al*., 2001). For MLH1 analysis, acrocentric SCs were identified using cenM-FISH probes, following a protocol described elsewhere (Oliver-Bonet *et al*., 2003).

Measurements and statistics

The number and position of RPA and MLH1 foci were recorded using the MicroMeasure program (MicroMeasure, Colorado State University, CO, USA, available at http://www.colostate.edu/Depts/Biology/MicroMeasure).

Gamma model was used for the distribution analysis of RPA and MLH1 interfocus distances. The statistic computer software SAS (Statistical Analysis Systems 9.1) was used for most statistical tests. Maximum likelihood method was used to generate a first estimate of two parameters and their 95% likelihood confidence interval for the predicted gamma distribution. The distribution of distances was then compared with the interference parameter (ν) of the predicted gamma distribution using the Kolmogorov–Smirnov one-sample goodness-of-fit test.

Results

For this study, at least 50 spermatocyte nuclei were captured and analysed per sample and per experiment. Spermatocytes were classified as leptotene, zygotene and pachytene according to the pairing status of the homologues. Pachytene nuclei were classified in substages according to sex body morphology (Solari, 1980; Codina-Pascual *et al*., 2005). As expected from previous studies, RPA foci were detected from early zygotene to mid-late pachytene. At zygotene, RPA was detected forming bridge-like structures between as yet unsynapsed homologues (Fig. 1a). These structures were more frequently seen at early zygotene, although they could also be observed at later stages of zygotene (Fig. 1b). In some cases, the bridge-like structures were located in regions where the distance between homologous chromosomes had been diminished (Fig. 1b and c). Association of

Table I. Average number and density of RPA and MLH1 foci for acrocentric chromosomes.

	Number of SCs analysed		Average number of foci (q arm) ($\pm$ SD)/range		Density of foci (foci per micrometre)	
	RPA	MLH1	RPA (early pachytene)	MLH1 (pachytene)	RPA	MLH1
SC 13	52	413	14.63 ($\pm$5.36)/5–26	1.87 ($\pm$0.45)/0–3	1.44	0.18
SC 14	47	413	13.76 ($\pm$4.94)/5–26	1.88 ($\pm$0.45)/0–3	1.28	0.17
SC 15	49	412	12.96 ($\pm$4.65)/5–26	1.88 ($\pm$0.43)/0–3	1.13	0.16
SC 21	51	411	4.98 ($\pm$2.06)/2–11	0.97 ($\pm$0.28)/0–2	1.33	0.26
SC 22	42	411	5.55 ($\pm$1.90)/2–10	1.14 ($\pm$0.41)/0–2	0.98	0.20

RPA with axial elements out of the context of the observed bridges was also observed (Fig. 1c).

The numbers of RPA and MLH1 foci were noted (Table I). At early pachytene stages, RPA foci in acrocentric chromosomes were found in apparently consistent patterns, with hot and cold spots for RPA localization (Fig. 2a). Distribution of RPA along the SCs was compared with MLH1 distribution; cumulative frequencies have been used for this purpose (Fig. 3a). Differences from the diagonal (which indicates uniform distribution of the cumulative frequencies along the SC) have been represented in charts (Fig. 3b). Differences from the slope of the diagonal line (expected uniform distribution) indicate the regions where RPA and MLH1 foci are detected more or less frequently than expected. Tendency of deviation from the diagonal is similar for both proteins and the pattern observed for RPA concurs with the pattern observed for MLH1 in numerous regions (overlapped areas Fig 3b).

The Kolmogorov–Smirnov test was used to determine the goodness-of-fit of MLH1 and RPA data to the gamma distribution. Results are shown in Table II. Although gamma distributions visually suit RPA distributions in most cases (Fig. 4), goodness-of fit between the observed distribution of RPA foci and the predicted gamma distribution was not statistically accepted for chromosomes 13, 14 and 15 ($P < 0.05$). MLH1 foci, on the other hand, statistically fit the gamma model except for chromosome 15.

FISH analysis showed that RPA was absent from the non-centromeric heterochromatic region of chromosome 9 (Fig. 1d). It was, however, present in 15–20% of the p arms of acrocentric chromosomes (Fig. 1e–f). Finally, at pachytene, the number of RPA foci was found to increase with chromosome length for the analysed chromosomes, except for chromosome 22 (Fig. 5).

Discussion

Analysis of the RPA protein has allowed the visualization of bridge-like structures that promote direct interactions between homologues by linking their axial elements at the zygotene stage (Fig. 1). *In vitro* experiments have indicated that assembly of RAD51 on ssDNA and subsequent homology search and strand exchange is stimulated in the presence of RPA (Sung and Robberson, 1995; Sugiyama *et al*., 1997). The actual model for the repair of DSBs *in vivo* proposes an ordered assembly of proteins wherein RPA goes first, followed by RAD52 and RAD51 (Symington, 2005): rAD52 displaces RPA from the ssDNA, allowing formation of the RAD51 nucleoprotein filament. The discovery of RPA nucleoprotein filaments between two homologues suggests that, in humans, RPA is still present on the nucleoprotein filament at the homology search stage. According to this observation, we propose that in human male meiosis, RPA plays a pre-synaptic role in the homology search and that this process occurs at the beginning of zygotene.

Visualization of pre-synaptic filaments of RPA (RPA bridges) also suggests that, in humans, the homology search precedes synapsis. In addition to their role in the homology search, these nucleoprotein filaments would also connect axial elements together, facilitating the subsequent synapsis of homologous chromosomes through the formation of the SC. A model that links meiotic recombination and the sites of SC initiation has already been suggested (Zickler *et al*., 1992; Fung *et al*., 2004; Henderson and Keeney, 2005). In this model, late recombination nodules also mark the sites of SC initiation. Comparison with MLH1 distribution (a marker for later recombination nodules, LNs) suggests that RPA and MLH1 have a similar distribution pattern, with coincidences at specific regions on the SCs (Fig. 3b). These specific sites where an excess of RPA and, later on the meiotic process, MLH1 accumulate could become recombination

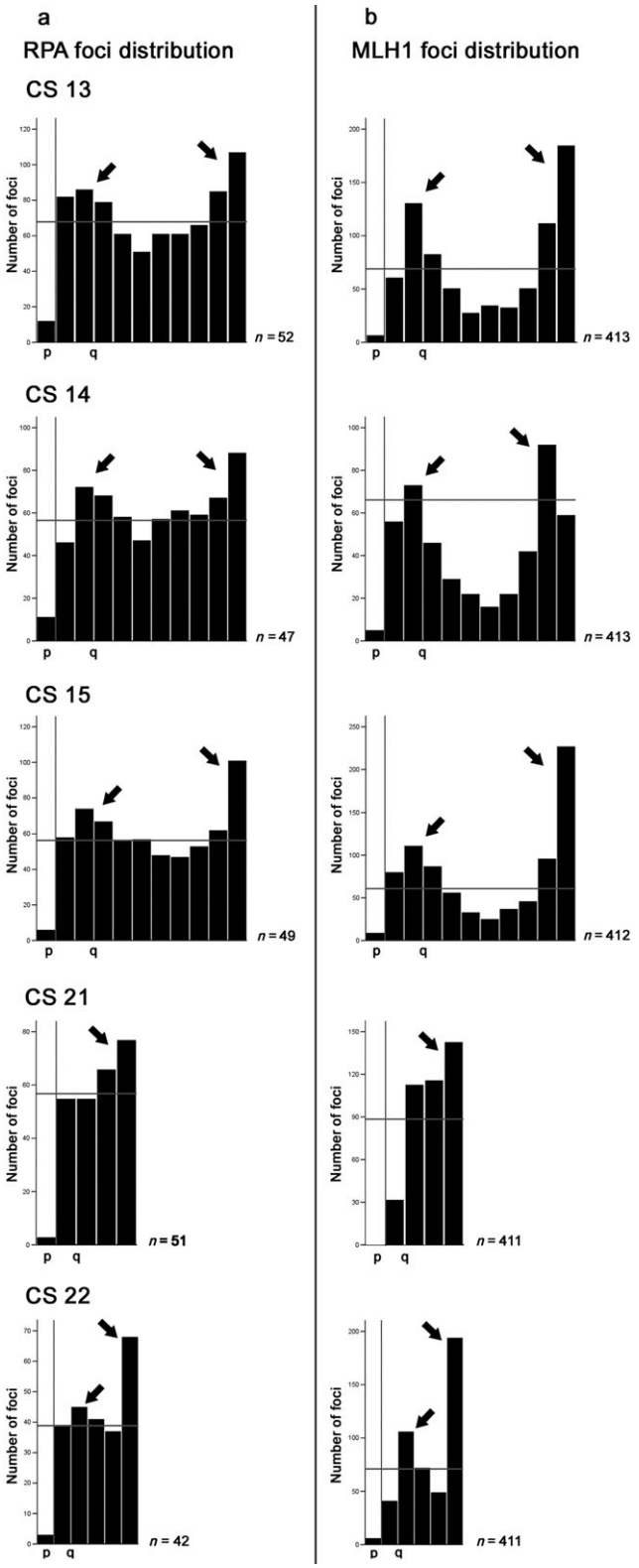

Figure 2: RPA and MLH1 foci distribution in the acrocentric chromosomes *Y*-axis indicates the total number of foci found in a given region. Bars represent SC divisions of about 1 μm of length and indicate the probability of a given RPA (**a**) or MLH1 (**b**) focus to be found in that particular region. Centromere position is indicated by a vertical line. The horizontal line represents the equal-probability value (i.e. the value expected if focus distribution was a random process). Distributions above this line indicate hot-spots for RPA or MLH1 (arrows), whereas distributions below it indicate cold-spots for these proteins. RPA and MLH1 display similar allocations of hot and cold spots in the analysed SCs.

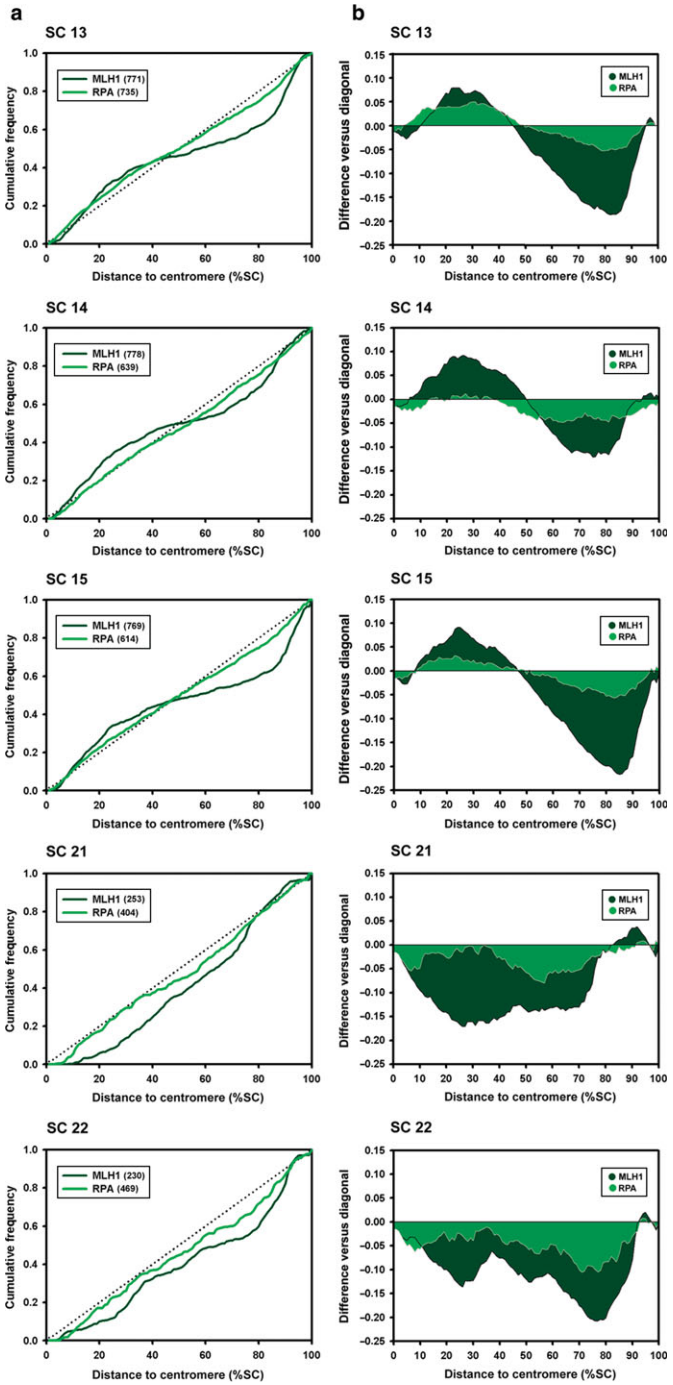

Figure 3: Distribution of RPA and MLH1 foci along the SCs
Cumulative frequencies of foci are represented in (**a**). Distances to the centromere are expressed as percentages of the SC length. Number of foci represented per protein can be found on the upper left corner of each chart, beside the protein's name. Differences from the diagonal have been charted in (**b**). Overlapped areas indicate regions where both RPA and MLH1 foci are detected either more or less frequently than the expected uniformed distribution (diagonal). Differences from the slope of the diagonal line indicate regions where RPA and MLH1 foci are more or less frequently detected.

hot spots later in the meiotic process. (Fig. 2a and b, Table I). These hot spots localize preferentially in subtelomeric regions (Codina-Pascual *et al*., 2006a; Sun *et al*., 2006), and the initiation of synapsis has been observed in these subtelomeric regions in human males (Brown *et al*., 2005). All these facts add evidence for a relationship between crossover localization and the initiation of synapsis.

Table II. Interference among MLH1 and RPA foci in human spermatocytes.

Focus type	Chromosome number	Number of interfocus distances	Interference parameter ν (CI)*	P**
MLH1	13	355	14.5 (12.5–16.8)	0.094
	14	360	16.4 (14.1–19.1)	0.066
	15	357	13.1 (11.3–15.1)	0.005*
	21	10	7.8 (3.3–18.3)	>0.250
	22	59	11.7 (8.2–16.7)	>0.250
RPA	13	704	2.2 (2.0–2.5)	0.002*
	14	592	2.4 (2.2–2.7)	0.003*
	15	571	2.1 (1.9–2.4)	0.006*
	21	204	2.9 (2.5–3.6)	0.085
	22	188	2.3 (1.9–2.8)	0.243

*Maximum likelihood estimated for the interference parameter ν in the gamma model (with estimated 95% CI).
**Estimated P-value (Kolmogorov–Smirnov goodness-of-fit test). The estimate of P is based on the deviance of the observations from the values expected based on the gamma equation with parameter ν.

FISH analysis showed that RPA was absent from the non-centromeric heterochromatic region of chromosome 9 (Fig. 1d). It was, however, present in 15–20% of the p arms of acrocentric chromosomes (Fig. 1f). It has been proposed that a reduction in crossing over is a typical feature of heterochromatic regions (Codina-Pascual *et al*., 2006b). During meiosis, heterochromatic regions are densely compacted (Stack, 1984). Therefore, recombination proteins may have reduced accessibility to heterochromatin due to this compact chromatin structure. The absence of RPA from the non-centromeric heterochromatic region of chromosome 9 may indicate that DSBs are not produced in this region (Fig. 1d). RPA foci, on the other hand, can be found in the short arm of the acrocentric chromosomes (Fig. 1f). The presence of RPA foci in the short arms of the acrocentric chromosomes indicates that a certain amount of recombination is taking place in these regions. Moreover, the fact that MLH1 foci have been detected in these regions indicates that a few of the recombination events are being resolved as crossovers.

RPA has been described as a member of both early (ENs) and transition nodules (TNs) (Plug *et al*., 1998; Moens *et al*., 2002). In an earlier study, Anderson *et al.* (2001) proposed that distribution of distances between adjacent ENs in plants, Coprinus, Bombyx and humans was random. The authors suggested the existence of two different population of ENs according to their composition and function. One population would associate with axial elements, collaborating in the first steps of synapsis. The second population would bind only to already synapsed elements and would be necessary for recombination events. It has also been proposed that TNs represent the link between ENs and LNs (Moens *et al*., 2002). If we assume that some TNs will become LNs, from the data obtained in the analysis of acrocentric chromosomes we could expect a ratio of approximately one LN for every seven TNs in the D group and one LN for every five TNs in the G group (Table I). Presence of RPA in both ENs and TNs supports the idea that the role of RPA extends from before synapsis until the later stages of recombination. As in the case of plants, behaviour observed for RPA in this work and data presented in the literature (Plug *et al*., 1998; Moens *et al*., 2002; Oliver-Bonet *et al*., 2005) also suggests the existence of two RPA focus populations. This may indicate a double role for this protein: an earlier role during homology search or synapsis initiation and a later role in recombination. Interaction of other proteins with RPA usually produces a modulation of the enzymatic activities of the proteins:

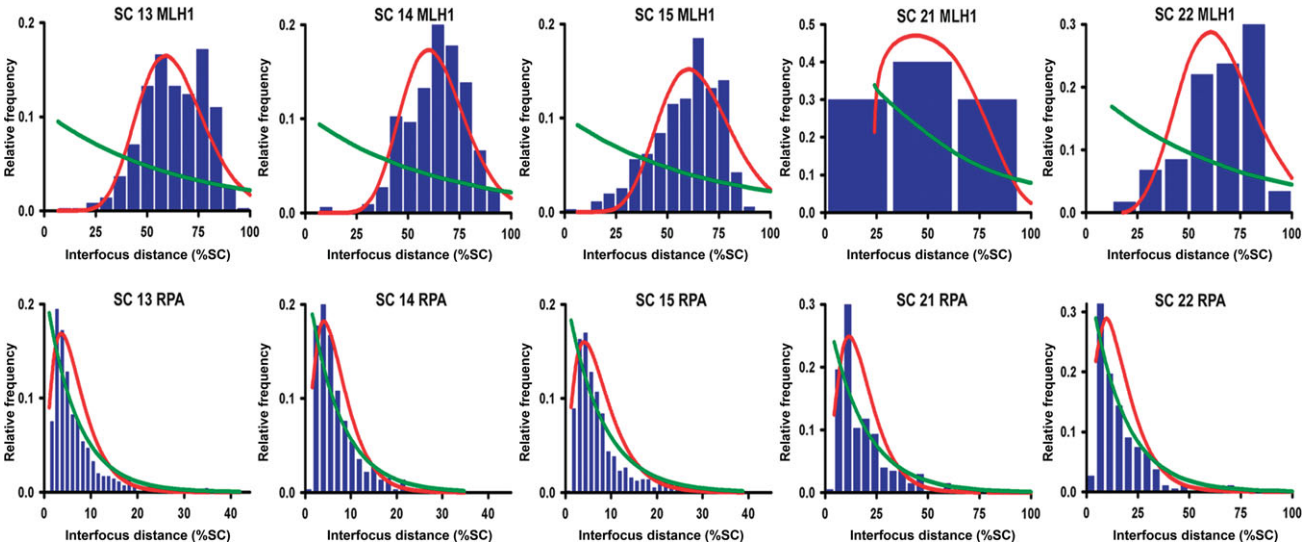

Figure 4: Histograms of observed interfocus distances of MLH1 and RPA for the acrocentric chromosomes in human spermatocytes
Visually, gamma distribution (red curve) fits better to the observed distribution, although this fit is only supported by the goodness-of-fit test in the SCs that have smaller numbers of analysed interfocus distances.

interactions between RPA and human RecQ DNA helicases, for instance, stimulate the unwinding of stretches of DNA (Brosh *et al*., 2000; Constantinou *et al*., 2000). Recent studies indicate that RPA interactions with p53 (Romanova *et al*., 2004) and with Mec1 in yeast (Bartrand *et al*., 2006) may function as controllers of homologous recombination. Such a huge repertoire of functions is not easy to explain. It could be that interactions with different proteins accounts for the different RPA behaviours.

Although RPA distribution resembled MLH1 distribution and apparently fit to a gamma model (Fig. 4), only samples with a small

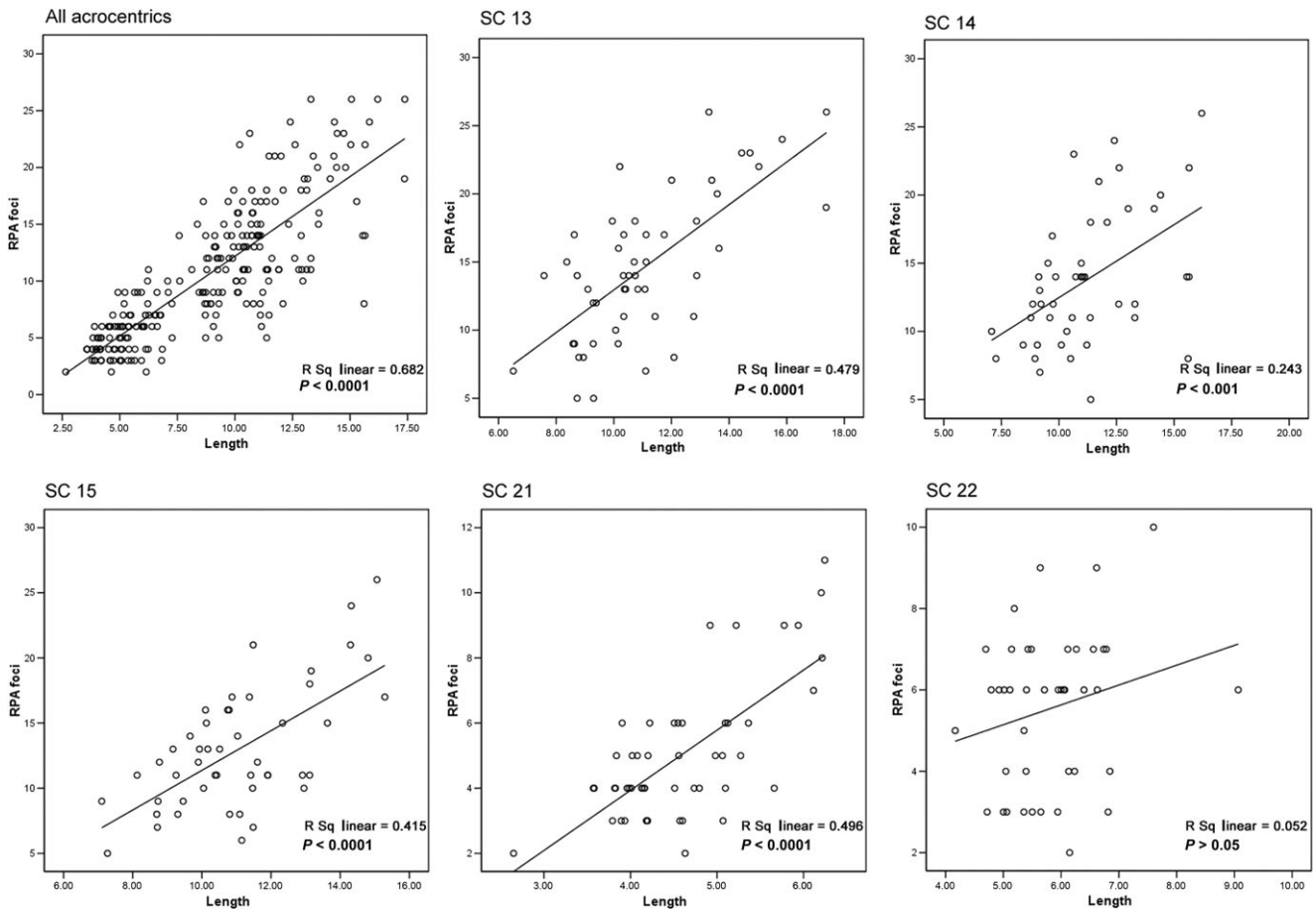

Figure 5: Correlations between SC length variation and the number of RPA foci for all acrocentric chromosomes, as a group and individually

number of observed RPA interfocus distances statistically agree to the gamma model (i.e. chromosomes 21 and 22). As the sample number increases, RPA distribution loses its correspondence to a gamma distribution (as shown by *P*-values). In their discussion, de Boer *et al*. (2006) suggest that sample size is critical for focus distribution to be adjusted to a gamma model. They propose that although interference mechanisms may conform to a gamma model, other factors may also influence focus distribution along the synaptonemal complexes. These factors, however, would have to affect RPA and MLH1 foci differently, as the two proteins' distributions differ in the goodness-of-fit to a gamma distribution (Table II).

Finally, at pachytene, the number of RPA foci was found to increase with chromosome length for the analysed chromosomes, except for chromosome 22.

Covariation between SC length and the number of crossover events has been observed in the analysis of LNs (MLH1 analysis) in human males by several authors (Lynn *et al*., 2002; Sun *et al*., 2004). The fact that early pachytene RPA focus numbers also covary with SC length supports the model in which SC length depends on the number of DSBs. In other words, the length of a given SC depends on the number of recombination events that are initiated in that particular SC, rather than the number of recombination events that become crossover sites. Allelic variation, affecting the loci encoding for different proteins upstream of the recombination pathway, has been suggested as a possible explanation for these results (Lynn *et al*., 2002).

Improving understanding of the relationship between RPA and other proteins will help in the comprehension of the meiotic process. Further experiments will be needed in order to assess the exact role of RPA in ENs, TNs and LNs.

Acknowledgements

We thank Jordi Benet for his valuable comments on the manuscript. We also thank T. Ashley, M. Fritzler and P. Moens for the generous gift of antibodies and the patients for their participation in the study. R.H.M. holds the Canada Research Chair in Genetics. M.O.B is recipient of CIHR Strategic Training Fellowships in Genetics, Child Development and Health.

Funding

This work was supported by grant MA-7961 from the Canadian Institutes of Health Research (CIHR).

References

Anderson LK, Hooker KD, Stack SM. The distribution of early recombination nodules on zygotene bivalents from plants. *Genetics* 2001;**159**:1259–1269.

Barlow AL, Benson FE, West SC, Hulten MA. Distribution of the Rad51 recombinase in human and mouse spermatocytes. *EMBO J* 1997;**16**:5207–5215.

Bartrand AJ, Lyasu D, Marinco SM, Brush GS. Evidence of meiotic crossover control in Saccharomyces cerevisiae through Mec1-mediated phosphorylation of replication protein A. *Genetics* 2006;**172**:27–39.

Brosh RM Jr, Li JL, Kenny MK, Karow JK, Cooper MP, Kureekattil RP, Hickson ID, Bohr VA. Replication protein A physically interacts with the Bloom's syndrome protein and stimulates its helicase activity. *J Biol Chem* 2000;**275**:23500–23508.

Brown PW, Judis L, Chan ER, Schwartz S, Seftel A, Thomas A, Hassold TJ. Meiotic synapsis proceeds from a limited number of subtelomeric sites in the human male. *Am J Hum Genet* 2005;**77**:556–566.

Carpenter AT. Gene conversion, recombination nodules, and the initiation of meiotic synapsis. *Bioessays* 1987;**6**:232–236.

Choo KH, Earle E, Vissel B, Filby RG. Identification of two distinct subfamilies of alpha satellite DNA that are highly specific for human chromosome 15. *Genomics* 1990;**7**:143–151.

Codina-Pascual M, Campillo M, Kraus J, Speicher MR, Egozcue J, Navarro J, Benet J. Crossover frequency and synaptonemal complex length: their variability and effects on human male meiosis. *Mol Hum Reprod* 2006a;**12**:123–133.

Codina-Pascual M, Navarro J, Oliver-Bonet M, Kraus J, Speicher MR, Arango O, Egozcue J, Benet J. Behaviour of human heterochromatic regions during the synapsis of homologous chromosomes. *Hum Reprod* 2006b;**21**:1490–1497.

Codina-Pascual M, Oliver-Bonet M, Navarro J, Campillo M, Garcia F, Egozcue S, Abad C, Egozcue J, Benet J. Synapsis and meiotic recombination analyses: MLH1 focus in the XY pair as an indicator. *Hum Reprod* 2005;**20**:2133–2139.

Constantinou A, Tarsounas M, Karow JK, Brosh RM, Bohr VA, Hickson ID, West SC. Werner's syndrome protein (WRN) migrates Holliday junctions and co-localizes with RPA upon replication arrest. *EMBO Rep* 2000;**1**:80–84.

de Boer E, Stam P, Dietrich AJ, Pastink A, Heyting C. Two levels of interference in mouse meiotic recombination. *Proc Natl Acad Sci USA* 2006;**103**:9607–9612.

Eggler AL, Inman RB, Cox MM. The Rad51-dependent pairing of long DNA substrates is stabilized by replication protein A. *J Biol Chem* 2002;**277**:39280–39288.

Fung JC, Rockmill B, Odell M, Roeder GS. Imposition of crossover interference through the nonrandom distribution of synapsis initiation complexes. *Cell* 2004;**116**:795–802.

Henderson KA, Keeney S. Tying synaptonemal complex initiation to the formation and programmed repair of DNA double-strand breaks. *Proc Natl Acad Sci USA* 2004;**101**:4519–4524.

Henderson KA, Keeney S. Synaptonemal complex formation: where does it start? *Bioessays* 2005;**27**:995–998.

Keeney S, Giroux CN, Kleckner N. Meiosis-specific DNA double-strand breaks are catalyzed by Spo11, a member of a widely conserved protein family. *Cell* 1997;**88**:375–384.

Ko E, Rademaker A, Martin R. Microwave decondensation and codenaturation: a new methodology to maximize FISH data from donors with very low concentrations of sperm. *Cytogenet Cell Genet* 2001;**95**:143–145.

Lynn A, Koehler KE, Judis L, Chan ER, Cherry JP, Schwartz S, Seftel A, Hunt PA, Hassold TJ. Covariation of synaptonemal complex length and mammalian meiotic exchange rates. *Science* 2002;**296**:2222–2225.

McPeek MS, Speed TP. Modeling interference in genetic recombination. *Genetics* 1995;**139**:1031–1044.

Moens PB, Kolas NK, Tarsounas M, Marcon E, Cohen PE, Spyropoulos B. The time course and chromosomal localization of recombination-related proteins at meiosis in the mouse are compatible with models that can resolve the early DNA–DNA interactions without reciprocal recombination. *J Cell Sci* 2002;**115**:1611–1622.

Moens PB, Tarsounas M, Morita T, Habu T, Rottinghaus ST, Freire R, Jackson SP, Barlow C, Wynshaw-Boris A. The association of ATR protein with mouse meiotic chromosome cores. *Chromosoma* 1999;**108**:95–102.

Oliver-Bonet M, Liehr T, Nietzel A, Heller A, Starke H, Claussen U, Codina-Pascual M, Pujol A, Abad C, Egozcue J *et al.* Karyotyping of human synaptonemal complexes by cenM-FISH. *Eur J Hum Genet* 2003;**11**:879–883.

Oliver-Bonet M, Turek PJ, Sun F, Ko E, Martin RH. Temporal progression of recombination in human males. *Mol Hum Reprod* 2005;**11**:517–522.

Plug AW, Peters AH, Keegan KS, Hoekstra MF, de Boer P, Ashley T. Changes in protein composition of meiotic nodules during mammalian meiosis. *J Cell Sci* 1998;**111**:(Pt 4).413–423.

Plug AW, Peters AH, Xu Y, Keegan KS, Hoekstra MF, Baltimore D, de Boer P, Ashley T. ATM and RPA in meiotic chromosome synapsis and recombination. *Nat Genet* 1997;**17**:457–461.

Romanienko PJ, Camerini-Otero RD. The mouse Spo11 gene is required for meiotic chromosome synapsis. *Mol Cell* 2000;**6**:975–987.

Romanova LY, Willers H, Blagosklonny MV, Powell SN. The interaction of p53 with replication protein A mediates suppression of homologous recombination. *Oncogene* 2004;**23**:9025–9033.

Solari AJ. Synaptosomal complexes and associated structures in microspread human spermatocytes. *Chromosoma* 1980;**81**:315–337.

Stack SM. Heterochromatin, the synaptonemal complex and crossing over. *J Cell Sci* 1984;**71**:159–176.

Sugiyama T, Zaitseva EM, Kowalczykowski SC. A single-stranded DNA-binding protein is needed for efficient presynaptic complex formation by the Saccharomyces cerevisiae Rad51 protein. *J Biol Chem* 1997;**272**:7940–7945.

Sun F, Oliver-Bonet M, Liehr T, Starke H, Ko E, Rademaker A, Navarro J, Benet J, Martin RH. Human male recombination maps for individual chromosomes. *Am J Hum Genet* 2004;**74**:521–531.

Sun F, Oliver-Bonet M, Liehr T, Starke H, Turek P, Ko E, Rademaker A, Martin RH. Variation in MLH1 distribution in recombination maps for individual chromosomes from human males. *Hum Mol Genet* 2006;**15**:2376–2391.

Sung P, Robberson DL. DNA strand exchange mediated by a RAD51-ssDNA nucleoprotein filament with polarity opposite to that of RecA. *Cell* 1995;**82**:453–461.

Symington LS. Focus on recombinational DNA repair. *EMBO Rep* 2005;**6**:512–517.

Turek PJ, Ljung BM, Cha I, Conaghan J. Diagnostic findings from testis fine needle aspiration mapping in obstructed and nonobstructed azoospermic men. *J Urol* 2000;**163**:1709–1716.

Walpita D, Plug AW, Neff NF, German J, Ashley T. Bloom's syndrome protein, BLM, colocalizes with replication protein A in meiotic prophase nuclei of mammalian spermatocytes. *Proc Natl Acad Sci USA* 1999;**96**:5622–5627.

Zickler D, Moreau PJ, Huynh AD, Slezec AM. Correlation between pairing initiation sites, recombination nodules and meiotic recombination in Sordaria macrospora. *Genetics* 1992;**132**:135–148.

Submitted on July 4, 2007; accepted on September 20, 2007